EUROPEAN ORGANIZATION FOR NUCLEAR RESEARCH

BA/HR/ml

CERN PS/84-13 (AA)

PLASMA LENS FOR THE CERN ANTIPROTON SOURCE

L. De Menna, G. Miano
Dipartimento Elettrico per l'Energia, Naples University, Italy

B. Autin, F. Boggasch, K. Frank, H. Riege
PS Division, CERN, CH-1211 Geneva, Switzerland

Paper presented at the 4th National Congress of Quantum Electronics and Plasma Physics, Capri, 21-23 may 1984, Italy.

Geneva, Switzerland
May 1984

Abstract

The work described in this paper aims at using the dynamic z-pinch as a magnetic lens system in particle accelerators. A cylindrical plasma lens is a linear pinch in which the current flows along the cylinder axis and the magnetic field is poloidal. The magnetic field inside the plasma column constitutes a linear lens for the particles. A plasma lens is under development for focusing large emittance antiproton beams in the future CERN Antiproton Collector (ACOL). Its principal characteristics are: a pinch radius of 10 to 15 mm, a plasma column length of 250 mm, a peak current of 500 kA, and a pulse duration of 4 to 5 μs. A possible plasma lens charging circuit, using saturable inductors as switches and the experimental results obtained at CERN with a prototype lens and pulse generator are presented.

1. INTRODUCTION

The antiproton beam emitted by a target has too wide a divergence to be accepted by a particle transport channel made of conventional iron quadrupoles. The insertion of a high magnetic field gradient device between the target and the entrance to the transport channel is therefore necessary. Essentially two types of devices are considered for this function. One is the so-called "lithium lens" (1, 2), which consists of a rod of solid lithium surrounded by a structure which withstands the large forces exerted by the thermal shock and the magnetic field associated with the large current. The other solution, described in this paper, is a "plasma lens" (3, 4, 5), which has the intrinsic advantages of being fully transparent to antiprotons and of being unaffected by radioactivity and mechanical pressure. In the Brookhaven plasma lens, developed in the early 60's and used for the neutrino beam line, a decrease in the divergence of the secondary meson beam and therefore an increase in the neutrino flux at the detector was obtained. The discharge was controlled using a solenoidal magnetic field but the lifetime of the lens was only of 24 hours (4).

A uniform current density can be generated in a linear pinch by discharging a high voltage capacitor bank between two electrodes in a low pressure gas. The magnetic field within the plasma, during the pinch phase, produces strong focussing of antiprotons travelling along the lens axis. The initial low-density plasma produced by pre-ionization, is assumed to have a large conductivity so that its skin depth is much less than the radius of the

plasma column. Thus the current flows in a thin shell on the surface of the plasma. When the current flow is sufficiently large so that the inward magnetic pressure exceeds the outward kinetic pressure of the gas, the current shell begins to collapse inwards. During the equilibrium pinch phase, when the plasma column reaches its minimum radius, a uniform current density, for a sufficient period of time, can be achieved.

A plasma lens is under development for focussing large emittance antiproton beams in the future CERN ANTIPROTON COLLECTOR (ACOL). In section 2 the beam optics of the linear lens is considered, in section 3 a pulse forming network, using saturable inductors as switches is described and in section 4 the experimental results obtained at CERN with a prototype lens and pulse generator are presented.

2. BEAM OPTICS IN A PLASMA LENS

The antiproton beam has an axial symmetry and is completely defined by its radius r and its divergence . The design of the focussing scheme drawn in Figure 1 consists in determining the length of the drift space f and of the lens l, the radius R of the pinched plasma columns and the plasma current I_p to match the

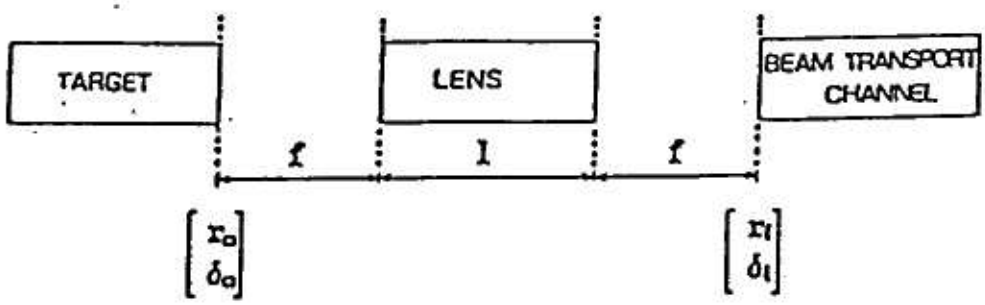

Fig. 1.

vector (r_o, δ_o) at the end of the target to the vector (r_1, δ_1) at the entrance to the channel. Under the assumption of a linear focussing lens, it can be proven (see Appendix) that the minimum current I_{th} necessary to focus the beam is given by

$$I_{th} = \frac{p}{e} \frac{2\pi}{\mu_o} \delta_o^2$$

where e is the electron charge, p the particle momentum and μ_o the vacuum permittivity ($4\pi \cdot 10^{-7}$). This minimum value corresponds to a zero drift length. For a finite value of f, the current is higher and such that:

$$\frac{I_{th}}{I_p} = 1 + \left[\frac{r_1}{r_o}\right]^2 - \left[\frac{R}{r_o}\right]^2$$

Inside the lens, the particles undergo an oscillation for which a phase φ can be defined:

$$\varphi = \frac{\delta_0 l}{R} \sqrt{\frac{I_p}{I_{th}}}$$

The lengths l and f are then given by the expressions:

$$l = \frac{r_0}{\delta_i} \varphi \sin\varphi \qquad f = \frac{r_0}{\delta_i} \cos\varphi$$

The parameters, which are aimed at for the ACOL project, are:

r_0 = 3 mm	δ_0 = 70 mrad	r_i = 21 mm	δ_i = 10 mrad	p = 3,5 GeV/c
f = 15 cm	l = 27 cm	R = 21 mm	I = 400 kA	$\phi = \pi/3$

3. THE SATURABLE INDUCTORS

In this section we describe a pulse generator based on the non-linear properties of the saturable inductors (6, 7). Saturable inductors or magnetic switching devices have cores of materials with rectangular B-H characteristics such as to saturate at very low values of the magnetizing force H, 10 to 50 A/m. For small values of the magnetizing force H, the saturable inductor has a high inductance, 100 to 1000 μH, while when the magnetic material saturates, the inductance falls to a very low value, 10 to 100 nH. Because of the large change in inductance, the saturable inductor may be used as a switching device. The principal advantages of the magnetic switches are the long lifetime, the fast switching time (10^{12} A/s) and the simplicity of the circuits. The principal disadvantage is that a special and expensive core material is required. The electrical scheme of the pulse generator we have designed is shown in fig. 2. In the last cell of the discharge circuit the magnetic core is incorporated between the quartz tube and the return current conductor. In the electrical equivalent circuit we can consider the plasma lens with incorporated magnetic core like a saturable inductor, P_1. The saturable inductor P_2 is designed so that the change in the flux induced in its core by the voltage across C_2 causes saturation when it is at the maximum value V. Then if we assume $C_1 = C_2 = C$ and if the saturated inductance of P_2 is smaller than L a fast oscillatory discharge takes place between C_2 and C_1 and approximately at half-period of the oscillation all the energy which was stored in C_2 has been transferred to C_1. The thickness d of the

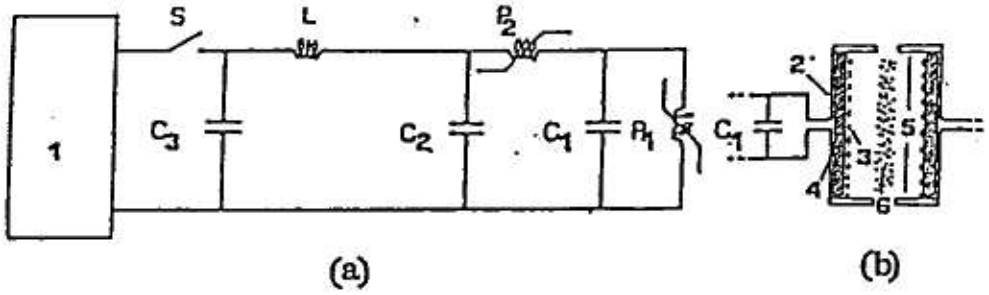

Fig. 2. Equivalent electrical circuit of the pulse generator a) and its last cell b)plasma lens with magnetic core.
1) dc-charging circuit; 2) return current conductor; 3) quartz tube; 4) magnetic core; 5) electrodes; 6) plasma current.

magnetic core surrounding the quartz chamber can be chosen such that C_1 discharge into the plasma lens at the moment of maximum charge. Neglecting hysteresis, eddy-currents and copper losses, assuming pre-magnetization for the saturable inductor, the thickness d is given by (8):

$$d = \frac{\pi\sqrt{2}}{81 B_s} l_p \sqrt{L_{1s} L_{2s}}$$

where l is the length of the lens, B_s is the magnetic field at the saturation inside the core, L_{1s} is the inductance of the plasma lens when the magnetic core is in the saturated state and Ip is the required peak plasma current. For economic and technical reasons the core of the saturable inductors P_1 and P_2 must have a minimum volume. To minimize the core volume of P_1, from the expression of the thickness d, it turns out that the values of L_{1s} and L_{2s} have to be kept as small as possible. Therefore the capacitor C_2 must be near the capacitor C_1. At last to minimize the core volume of P_2 the charge of C_2 must be quick and therefore we need another capacitor bank C_3 with a normal switch near the dc-charging circuit.

4. EXPERIMENTAL RESULTS

A small plasma lens prototype model with pseudospark geometry (9) and a quartz tube of 200 mm length and 40 mm inner diameter has been studied in a 20 kJ capacitor discharge circuit (V_c = 12 kV, i_{max} = 200 kA). The main objects of concern were: the energy dissipation in the lens, the influence of pre-ionization on breakdown delay and jitter, the pinch dynamics, the stability of the discharge and the verification of scaling laws needed for the layout of a lens for antiproton focusing.

Waveform measurements of the current through and the potential difference across the plasma lens not only provide information on energy loss, but also on breakdown delay, pinch dynamics and stability. The breakdown delay τ_B , which is a function of pressure, can be reduced by a factor of 5 with a weak (1mA) preionization of the lens. In Ar above 0.5 mb the delay τ_B is less than 20 ns. To minimize initial energy losses a strong pre-ionization was applied by the leakage current (10-100 A) through a series saturable inductor which saturates after 1 μs (10).

The internal resistance averaged over the first half wave measures between 10 and 15 mΩ. Figure 3 shows typical waveforms for Ar at 4 mb. The voltage peak and the dip in current waveform correspond to the first contraction phase of the pinch (τ_{pinch}).

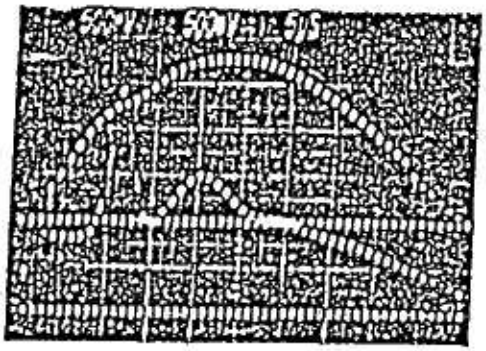

Fig. 3. Current (top) and diff. voltage (bottom) waveforms for Ar at 4 mb, V_c = 5 kV (19 kA/div, 0.5 kV/div).

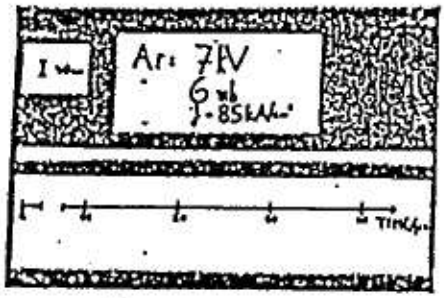

Fig. 4. Streak photograph of first contraction phase.

A more detailed study of pinch dynamics and stability was performed with a streak camera (11). Streak (Fig. 4) and framing photographs show stability during the pinch phase for more than the required 500 ns. Pinching time τ_{pinch} and minimum pinch radius R_{pinch} were measured as functions of pressure p (Fig. 5), current rise di/dt, and atomic number A for He, Ar, N_2, Xe and Xe/He, He/Ar mixtures as filling gases. The relative validity of the magneto-hydrodynamical scaling law for the pinch time $\tau_{pinch} \sim (Ap)^{1/4} (di/dt)_0^{-1/2}$ was verified and for R_{pinch} an empirical relationship was found.

5. DISCUSSION AND FUTURE PLANS.

By extrapolation from these first prototype results we are now able to design a new prototype lens where the pinching phase coincides with the current maximum and dR_{pinch}/dt and di/dt are zero. This favours stable conditions for focusing. When the time to pinch, τ_{pinch}, and the pinch radius, R_{pinch}, are fixed, only pressure p and inner radius r_0 of the quartz tube are free parameters to define the pinch dynamics. The next stage of plasma lens

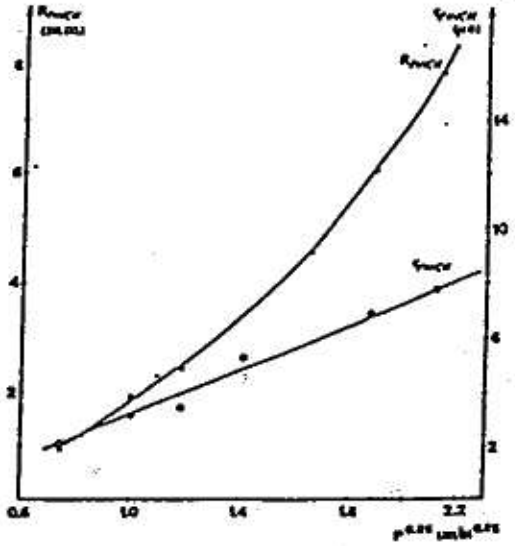

Fig. 5. Pinch radius and time as function of pressure (Ar). Pulse energy ≈ 17 kJ.

development aims at life tests of a new prototype under realistic conditions: 1 pulse of 20 to 30 kJ every 3 to 5 s, V_c = 20 to 25 kV, half wave-length 10 to 12 μs, and i_{max} 450 to 500 kA. In order to obtain pinch radii of 10 to 15 mm at reasonable gas pressures a quartz tube radius of 160 to 200 mm will be required. This lens will be pulsed in a simple low inductance capacitor discharge circuit. A saturable inductor for strong pre-ionization will be incorporated. Presently a 250 mm diameter lens is studied in the old high inductance pulse generator. Pinch time τ_{pinch} and current maximum can be made to coincide at 10 kV charging voltage in Ar at 0.15 mb. After successful life testing a new plasma lens for real focusing of antiprotons will be incorporated into a pulse generator of the type described in sec. 3.

REFERENCES

(1) B. F. Bayanov et alter, Proceedings of the 12th Intern. Conference on high-Energy Accelerators, Fermilab, August 11-16, 1983.

(2) G. Biallas et alter, Proceedings of the 12th Intern. Conference on high-Energy Accelerators, Fermilab, August 11-16, 1983.

(3) W. Panofsky, W. Baker, Rev. Sci. Instr., 21 5(1950).

(4) F. B. Forsyth et alter, IEEE Trans. on Nucl. Science, June 1965, pp. 872 -876.

(5) F. Krienen, Fermilab-p̄-note 137, July 1981.

(6) W. S. Melville, Proc. IEE, 1951, vol. 98, pt. 3, pp. 185-207.

(7) W. C. Nunnally, LA - 8862 - MS, UC - 38, September 1981.
(8) L. De Menna, G. Miano, PS/ACOL/Note 84-5, 1984 CERN (Geneva).
(9) J. Christiansen, C. Schultheiss, Z. Phys. A 290 (1979) 35.
(10) E. J. Lauer, D. Birx, Proc. Power Mod. Symp., Baltimore, 1982, 47.
(11) J. Christiansen, K. Frank, H. Riege, R. Seeboeck, CERN/PS/84-10 (AA), 1984.

APPENDIX

BEAM OPTICS IN A LINEAR LENS

The beam characteristics are defined by the emittance ellipses (Fig. 1). The source-image mapping can be described using a matrix formalism which connects exit-to entrance transverse particle coordinates:

$$\begin{pmatrix} r_i \\ \delta_i \end{pmatrix} = M \begin{pmatrix} r_o \\ \delta_o \end{pmatrix}$$

The transfer matrix of a drift space is

(1) $$D = \begin{pmatrix} 1 & f \\ 0 & 1 \end{pmatrix}$$

The plasma lens has a focusing strength K equal to:

(2) $$K = \frac{e}{p} \frac{\mu_o j}{2}$$

Where e is the charge of the particle, p the momentum and j the current density. Its transfer matrix is

(3) $$P = \begin{pmatrix} \cos(\sqrt{K}\,l) & 1/\sqrt{K}\,\sin(\sqrt{K}\,l) \\ -\sqrt{K}\,\sin(\sqrt{K}\,l) & \cos(\sqrt{K}\,l) \end{pmatrix}$$

The total transfer matrix:

$$M = D\,P\,D$$

defines the required imaging if the drift length is chosen so that

(4) $$f = \frac{1}{\sqrt{K}\tan(\sqrt{K}l)}$$

In this case, M is written:

$$M = \begin{pmatrix} 0 & \frac{1}{\sqrt{K}\sin(\sqrt{K}\,l)} \\ -\sqrt{K}\sin(\sqrt{K}\,l) & 0 \end{pmatrix}$$

and

(5) $$\sqrt{K}\sin\sqrt{K}\,l = \frac{\delta_i}{r_o}$$

The radius of the plasma column results from beam envelope calculations which are conveniently performed using the Twiss parameters β, α, γ:

(6) $$\beta = \frac{r^2}{\epsilon} \quad , \alpha = -\frac{1}{2}\frac{d\beta}{dz} \quad , \gamma = \frac{1+\alpha^2}{\beta}$$

where ϵ is the beam emittance, r the beam radius and z the longitudinal coordinate. In a drift space, the Twiss parameters are transformed according to the relations:

$$(7) \qquad \beta_1 = \beta_0 + \frac{f^2}{\beta_0} \qquad \alpha_1 = \alpha_0 - \frac{f}{\beta_0} \qquad \gamma_1 = \frac{1+\alpha_1^2}{\beta_1}$$

and, along a focusing lens, β varies like:

$$(8) \qquad \beta = \frac{1+\cos(2\sqrt{K}z)}{2}\beta_1 - \frac{\sin(2\sqrt{K}z)}{\sqrt{K}}\alpha_1 + \frac{1-\cos(2\sqrt{K}z)}{2K}\gamma_1$$

so that its maximum value is:

$$(9) \qquad \hat{\beta} = \frac{1}{2}\left(\beta_1 + \frac{\gamma_1}{K}\right) + \sqrt{\frac{1}{4}\left(\beta_1 + \frac{\gamma_1}{K}\right)^2 - \frac{1}{K}}$$

By noting that the β value at the image point is:

$$(10) \qquad \beta_i = \frac{\epsilon}{\delta_i^2}$$

and substituting (7), (4) and (5) into (9), we get the relation

$$(11) \qquad \frac{1}{K} = \hat{\beta}\,(\beta_0 - \hat{\beta} + \beta_i)$$

with the condition:

$$(12) \qquad 0 < \hat{\beta} - \beta_i < \beta_0$$

The relation (11) can be used to choose the plasma current I. Let us define a threshold current:

$$(13) \qquad I_{th} = \frac{p}{e}\,\frac{2\pi}{\mu_0}\,\delta_0^2$$

so that the focusing strength can be written:

$$(14) \qquad K = \left(\frac{\delta_o}{R}\right)^2 \frac{I}{I_{th}}$$

where $R = \sqrt{\epsilon\hat{\beta}}$ is the radius of the lens. The equation (11) becomes:

$$(15) \qquad \frac{I_{th}}{I} = 1 + \left(\frac{r_i}{r_0}\right)^2 - \left(\frac{R}{r_0}\right)^2$$

It is helpful to optimize the lens parameters in terms of the phase of the particle oscillation inside the lens:

$$(16) \qquad \psi = \sqrt{K}\,l$$

Expressions (4) and (5) can be combined and rearranged to contain electrical and geometrical parameters only. They provide the formulae for the length of the drift space and the length of the lens:

$$f = \frac{r_0}{\delta_i} \cos\phi \tag{17}$$

$$l = \frac{r_0}{\delta_i} \phi \sin\phi \tag{18}$$

By replacing l and K by their expressions (18) and (14) in the definition of the phase (16), we get

$$\frac{I_{th}}{I} = \left(\frac{\delta_0 r_0 \sin\phi}{\delta_i R} \right)^2 \tag{19}$$

From (15) and (19), a biquadratic equation in $\frac{R}{r_0}$ can be drawn and its solution is:

$$R = \frac{r_0}{\sqrt{2}} \sqrt{1 + \left(\frac{r_i}{r_0}\right)^2 + \sqrt{\left[1 + \left(\frac{r_i}{r_0}\right)^2\right]^2 - 4\left(\frac{r_i}{r_0}\right)^2 \sin^2\phi}} \tag{20}$$

When ϕ is included between o and $\frac{\pi}{2}$, R belongs to the interval $\left(r_i, \sqrt{r_i^2 + r_0^2}\right)$

In practical cases, r_0 is small with respect to r_i and R is almost constant and equal to r_i.

Knowing R, the current I is given by:

$$I = \left(\frac{R}{r_i \sin\phi} \right)^2 I_{th} \tag{21}$$

In the approximation of a small value of r_0, I has the simple expression:

$$I = \frac{I_{th}}{\sin^2\phi}$$

The position $\hat{z}$ of the beam waist inside the lens results from the condition:

$$\frac{d\beta}{dz} = 0$$

applied to the relation (8). After some arithmetics using the formulae (13) to (19), the expression of $\hat{z}/l$ is

$$\frac{\hat{z}}{l} = \frac{1}{2\phi} \text{Atan} \frac{\sin 2\phi}{\left(\frac{r_0}{r_i}\right)^2 + \cos 2\phi}$$

$\frac{\bar{z}}{l}$ belongs to the internal $\left(\frac{1}{1+\left(\frac{r_0}{r_1}\right)^2} \cdot 1 \right)$ when ϕ varies from 0 to $\frac{\pi}{2}$

The variations of I, l, f and R are plotted in Figure 7 for typical parameters of the ACOL project. In contrast with the lithium lens which is limited in length because of the antiproton reabsorption, the plasma lens can work in the vicinity of the threshold current.

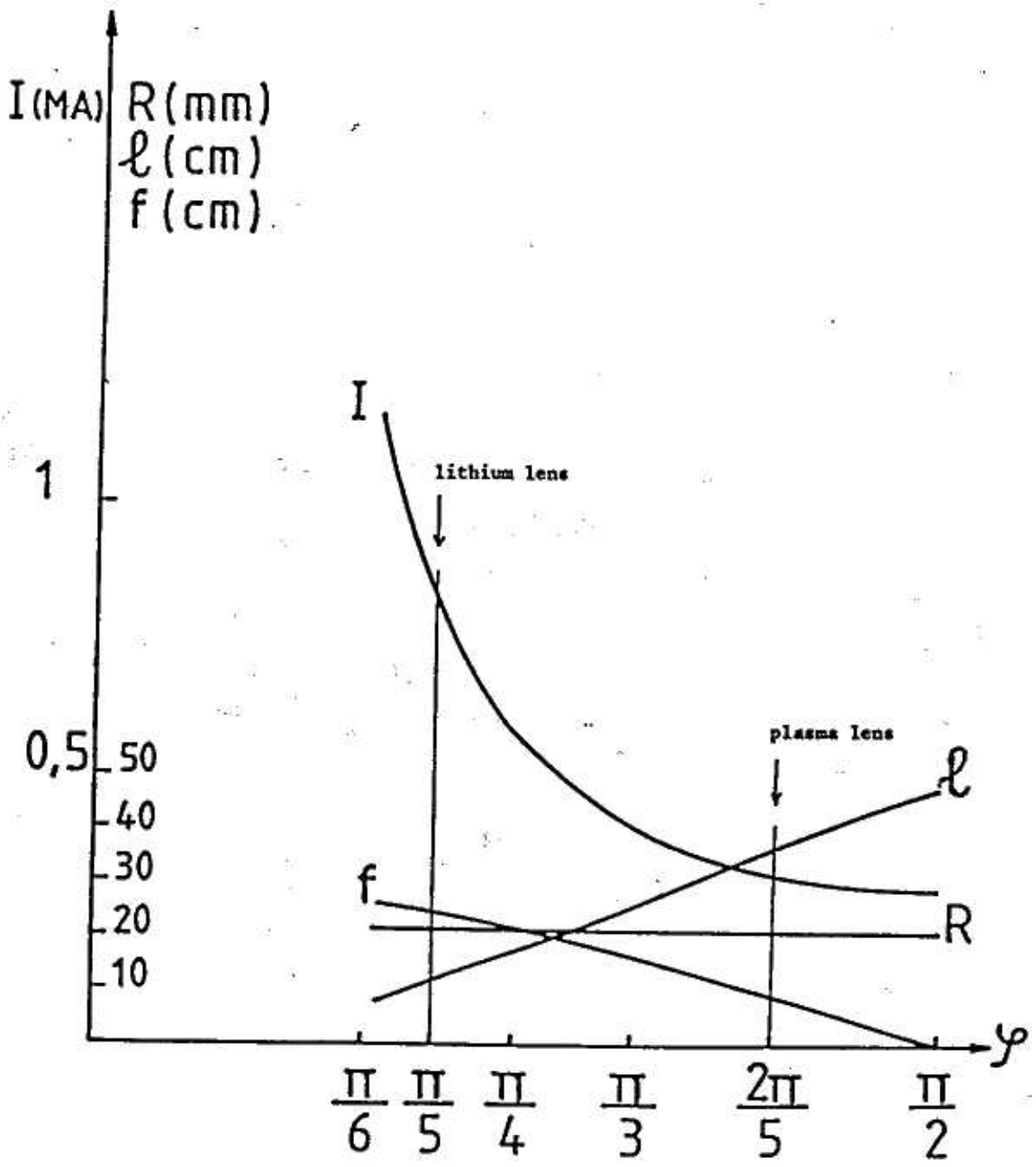

Figure 7. Variations of I, R, l and f versus ϕ